

A hybrid finite difference and integral equation method for modeling and inversion of marine CSEM data

Daeung Yoon, Michael S. Zhdanov, Hongzhu Cai, and Alexander Gribenko, University of Utah and TechnoImaging*

Summary

One of the major problems in the modeling and inversion of marine controlled source electromagnetic (MCSEM) data is related to the need for accurate representation of very complex geoelectrical models typical for marine environment. At the same time, the corresponding forward modeling algorithms should be powerful and fast enough to be suitable for repeated use in hundreds of iterations of the inversion and for multiple transmitter/receiver positions. To this end, we have developed a novel 3D modeling and inversion approach, which combines the advantages of the finite difference (FD) and integral equation (IE) methods. In the framework of this approach, we solve the Maxwell's equations for anomalous electric fields using the FD approximation on a staggered grid. Once the unknown electric fields in the computation domain of the FD method are computed, the electric and magnetic fields at the receivers are calculated using the IE method with the corresponding Green's tensor for the background conductivity model. This approach makes it possible to compute the fields at the receivers accurately without the need of very fine FD discretization in the vicinity of the receivers and without the need for numerical differentiation and interpolation. We have also developed an algorithm for 3D inversion of MCSEM data based on the hybrid FD-IE method. A model study for the 3D inversion of MCSEM data is presented to demonstrate the effectiveness of the developed hybrid method.

Introduction

The IE method represents one of the most effective numerical solvers for localized anomalous structures embedded in a layered earth. One of the advantages of the IE method is that it only requires a solution within the anomalous domain, and the electric and magnetic fields at the receivers are calculated based on the Green's tensor approach. The IE modeling domain includes inhomogeneous geoelectrical structures only and it is typically very small compared to the modeling domains of the differential equation (DE) methods, which require a large computational domain to satisfy to the corresponding boundary conditions. At the same time, the system matrix of the IE method is dense, so if the complexity of the model grows, the IE method requires significantly larger amount of computational memory and time.

The advantage of the DE method is the sparsity of the system matrices, which improves the condition number and makes the corresponding systems easier to solve compared to the IE method (Avdeev, 2005). However, the DE methods require a very large computational domain and extensive mesh refinement in the vicinity of the receivers to reduce errors caused by the interpolation and numerical differentiation required to calculate the electric and magnetic fields in the receivers. To avoid mesh refinement and/or numerical errors, Cox and Zhdanov (2014) applied the Green's tensor approach to the finite element (FE) method to calculate magnetic fields and their sensitivities at the receivers. In this paper, we use a similar concept of the Green's tensor approach, and apply it to the FD method.

The FD modeling algorithm is based on the staggered grid (Yee, 1966). Once the unknown electric fields in the computation domain of the FD method are computed, the electric and magnetic fields at the receivers are calculated using the IE method with the corresponding Green's tensor for the background conductivity model. This approach makes it possible to compute the fields at the receivers accurately without the need of very fine FD discretization in the vicinity of the receivers and without the need for numerical differentiation and interpolation.

The developed hybrid algorithm was incorporated as the forward EM modeling engine in a general regularized inversion scheme, based on the re-weighted conjugate gradient method. Although the inversion algorithm is general, this paper presents an application of this method specifically to the 3D inversion of marine controlled-source electromagnetic (MCSEM) data. A model study of the 3D inversion of synthetic MCSEM data is presented to demonstrate the effectiveness of the developed hybrid method.

Finite-difference modeling of the anomalous electric field

The implementation of the FD method developed in this paper follows that of Newman and Alumbaugh (1995) and Alumbaugh et al. (1996). The method solves Maxwell's equations in the frequency domain based on a finite-difference scheme on a staggered grid and uses the anomalous field formulation with the total field being decomposed into a background, \mathbf{E}^b , and anomalous, \mathbf{E}^a , fields. The magnetic permeability within the earth, μ , is

Hybrid FD-IE method for modeling and inversion

assumed to be constant, $\mu_0 = 4\pi \times 10^{-7}$ H/m everywhere, and the conductivity tensor, σ is considered to be diagonal.

A finite-difference representation of Maxwell's equations on a staggered grid can be written as a linear system of equations as follows:

$$\mathbf{K}\mathbf{e} = \mathbf{s}, \quad (1)$$

where \mathbf{e} is the unknown vector of the anomalous electric field, and \mathbf{s} is a vector containing the source terms. The matrix \mathbf{K} is sparse and a symmetric complex matrix composed of real numbers except for the diagonal elements. We use multifrontal massively parallel sparse direct solver, MUMPS (Amestoy et al., 2001, 2006), to solve the system of equations (1), which enables the solution of large-scale problems with multiple sources in an efficient manner.

Integral equation method for computing the EM field at the receivers

The conventional FD method requires an interpolation to calculate the electric fields at the receivers, a numerical approximation of the curl of the electric field, and an interpolation to calculate the magnetic fields at the receivers. Those numerical differentiation and interpolation can cause some numerical errors, and require mesh refinement in the vicinity of the receivers to reduce the errors. In order to avoid those problems, we use an IE approach to calculate the electric and magnetic fields at the receiver. The anomalous electric and magnetic fields at the receiver position, \mathbf{r}_j , can be expressed as an integral over the excess currents in the inhomogeneous domain \mathbf{D} :

$$\mathbf{E}^a(\mathbf{r}_j) = \iiint_{\mathbf{D}} \widehat{\mathbf{G}}_E(\mathbf{r}_j|\mathbf{r}) \Delta\sigma(\mathbf{r}) \cdot [\mathbf{E}^b(\mathbf{r}) + \mathbf{E}^a(\mathbf{r})] d\mathbf{v} \quad (2)$$

$$\mathbf{H}^a(\mathbf{r}_j) = \iiint_{\mathbf{D}} \widehat{\mathbf{G}}_H(\mathbf{r}_j|\mathbf{r}) \Delta\sigma(\mathbf{r}) \cdot [\mathbf{E}^b(\mathbf{r}) + \mathbf{E}^a(\mathbf{r})] d\mathbf{v} \quad (3)$$

where $\widehat{\mathbf{G}}_E(\mathbf{r}_j|\mathbf{r})$ and $\widehat{\mathbf{G}}_H(\mathbf{r}_j|\mathbf{r})$ are the electric and magnetic Green's tensors defined for an unbounded conductive medium with the normal (horizontally layered) anisotropic conductivity σ_{norm} ; the inhomogeneous domain \mathbf{D} represents a volume with the anisotropic anomalous conductivity distribution $\sigma(\mathbf{r}) = \sigma_{\text{norm}} + \Delta\sigma(\mathbf{r})$.

The volume integrals in equations (2) and (3) are calculated numerically using the integration over the cells of the discretization grid. In the case of the IE method, vector \mathbf{r} is located at the center of the cell where all three components of the electric fields are assigned. However, in the FD scheme based on the staggered grid, the electric fields to be solved are located at the edges of the cell. Therefore, the numerical formulas for the IE method should be modified accordingly, so that the vector \mathbf{r} should represent the points, $\mathbf{r}_x, \mathbf{r}_y$ and \mathbf{r}_z where the $x, y,$ and z components of the electric fields are located in the staggered grid, respectively.

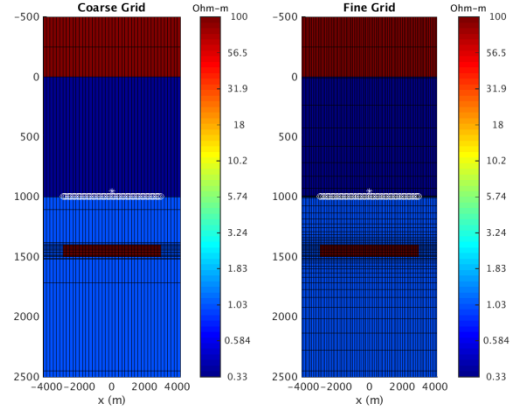


Figure 1: Model 1. A horizontally layered geoelectrical model with a coarse grid (left panel) and a fine grid (right panel). The isotropic resistive reservoir layer with a resistivity of 100 Ohm-m is embedded in the sediment below the seawater layer. The white star indicates the position of the electrical dipole source, and the white circles denote the receiver positions.

Obviously, the hybrid FD-IE method requires one additional computation of the Green's tensors at the midpoints of the cell edges in comparison with the conventional IE method. However, this complication can be overcome by pre-computing the Green's tensors and reusing them at every iteration of the inversion.

Verification of the hybrid FD-IE modeling method

In order to verify the accuracy and the efficiency of the hybrid FD-IE forward modeling method, it has been compared with three other techniques: (1) a 1D semi-analytical solution, (2) a conventional FD method, and (3) a 3D IE method.

Model 1 is a horizontally layered geoelectrical model with an isotropic resistive rectangular reservoir (Figure 1). The background is a seawater-sediment model with air-earth interface at $z = 0$ and a seawater depth of 1000 m. The resistivities of air, seawater, and sediments are 10^{-6} Ohm-m, 0.3 Ohm-m, and 1 Ohm-m, respectively. The electromagnetic field is excited by a horizontal electric dipole oriented in the x direction with a moment of 1 Am and located in the seawater with coordinates (0, 0, 950) m, which is 50 m above the sea floor. The frequency of the current in the transmitting dipole is 1 Hz. An isotropic 3D resistive rectangular reservoir with a resistivity of 100 Ohm-m is embedded in the sediments from a depth of 1400 to 1500 m and with a size of 3 km x 3 km x 100 m in the $x, y,$ and z directions, respectively. The volume of the 3D resistive reservoir is considered as a domain with anomalous conductivity.

Hybrid FD-IE method for modeling and inversion

We calculated the EM responses for Model 1 using two different grids (coarse and fine), and the responses were then compared with the 1D semi-analytical solution. For both grids, the FD modeling domains were selected as $\mathbf{D}_{FD} = \{-4 \text{ km} \leq x, y \leq 4 \text{ km}; -0.5 \text{ km} \leq z \leq 3 \text{ km}\}$ based on the skin depth. The coarse grid consisted of $41 \times 31 \times 21 = 26,691$ cells, with uniform cells of 200 m by 200 m in the x and y directions, and with logarithmically increasing cell size from the bottom of the reservoir (anomalous domain) to the boundaries of the FD domain in the z direction as shown in the left panel of Figure 1. The anomalous domain is discretized using a $200 \text{ m} \times 200 \text{ m} \times 10 \text{ m}$ uniform grid. In Figure 2, the anomalous electric fields computed by the hybrid FD-IE method and the conventional FD method are compared to the 1D semi-analytical solution based on the Hankel transform (Ward and Hohmann, 1988; Zhdanov and Keller, 1994). On this coarse grid, the hybrid FD-IE responses were in a good agreement with the semi-analytical solution, showing less than 3% relative errors, whereas the FD responses exhibited large discrepancies.

Next, we gradually increased the number of cells within the same FD modeling domain was increased as was done

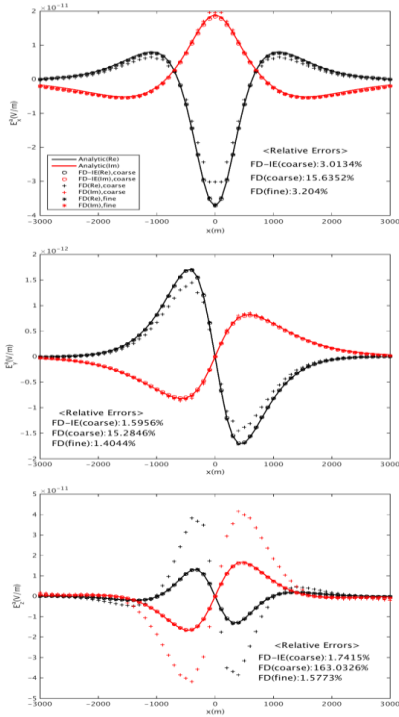


Figure 2: Model 1. A comparison of anomalous electrical fields computed using the hybrid FD-IE method, the FD method, and an 1D semi-analytic solution based on the horizontally layered model with an isotropic resistive reservoir layer. The top, middle, and bottom panels present the x, y, and z components of the anomalous electric field, respectively.

above for the coarse grid, and the grids surrounding the receivers were refined as well, until a grid was found for which the FD response was characterized by relative errors similar to those produced by the hybrid FD-IE method on the coarse grid. The fine grid, which was finally determined by this process, consisted of $81 \times 61 \times 52 = 256,932$ cells, with $100 \text{ m} \times 100 \text{ m}$ uniform grid in the x and y directions, a minimum cell size of 5 m near the receiver positions, and a maximum cell size of 250 m in the z direction, as shown in the right panel of Figure 2. Note that, in order to have the level of errors for the FD responses similar to those for the hybrids FD-IE responses on the coarse grid, we had to refine not only the grid in the vicinity of the receivers, but also the entire grid within the FD domain. We have also computed the fields using the hybrid FD-IE on the fine grid. The main conclusion is that the hybrid FD-IE method always provides the smaller errors than the conventional FD method, if the same discretization grids are used.

Inversion methodology

We have implemented the developed hybrid FD-IE modeling method in the algorithm of inversion of the MCSEM data following the paper by Gribenko and Zhdanov (2007). The regularized inversion algorithm is based on minimization of the Tikhonov parametric functional, (Tikhonov and Arsenin, 1977; Zhdanov, 2002):

$$P^\alpha(\Delta\sigma) = \|\mathbf{W}_d(\mathbf{A}_h(\Delta\sigma) - \mathbf{d})\|^2 + \alpha\mathbf{s}(\Delta\sigma) = \min \quad (4)$$

where \mathbf{d} is the vector of the observed data; $\mathbf{A}_h(\Delta\sigma)$ is the forward modeling operator for computing the predicted data based on the hybrid FD-IE method; and \mathbf{W}_d is the diagonal data weighting matrix formed by the inverse amplitudes of the background electric field.

The first term of the parametric functional (4) represents the weighted misfit functional, and the second term is the stabilizer. We apply the regularized conjugate gradient (RCG) algorithm of the parametric functional minimization, summarized as follows (Zhdanov, 2002):

$$\begin{aligned} \mathbf{r}_n &= \mathbf{A}_h(\Delta\sigma) - \mathbf{d}, \\ \mathbf{l}_n &= \mathbf{F}_n^* \mathbf{W}_d^* \mathbf{W}_d \mathbf{r}_n + \alpha \mathbf{W}_m^* \mathbf{W}_m (\Delta\sigma_n - \Delta\sigma_{appr}), \\ \beta_n &= \|\mathbf{l}_n\|^2 / \|\mathbf{l}_{n-1}\|^2, \\ \hat{\mathbf{l}}_n &= \mathbf{l}_n + \beta_n \hat{\mathbf{l}}_{n-1}, \hat{\mathbf{l}}_0 = \mathbf{l}_0, \\ \mathbf{k}_n &= (\hat{\mathbf{l}}_n, \mathbf{l}_n) / (\|\mathbf{W}_d \mathbf{F}_n \hat{\mathbf{l}}_n\|^2 + \alpha \|\mathbf{W}_m \hat{\mathbf{l}}_n\|^2), \\ \Delta\sigma_{n+1} &= \Delta\sigma_n - \mathbf{k}_n \hat{\mathbf{l}}_n, \end{aligned}$$

where \mathbf{F} is the Fréchet derivative matrix based on the quasi-Born (QB) approximation (Gribenko and Zhdanov, 2007), and \mathbf{W}_m is the weighting matrix of the model parameters determined based on the weighted Fréchet derivative matrix (sensitivities):

$$\mathbf{W}_m = \text{diag}(\mathbf{F}^* \mathbf{W}_d^* \mathbf{W}_d \mathbf{F})^{0.25}.$$

Hybrid FD-IE method for modeling and inversion

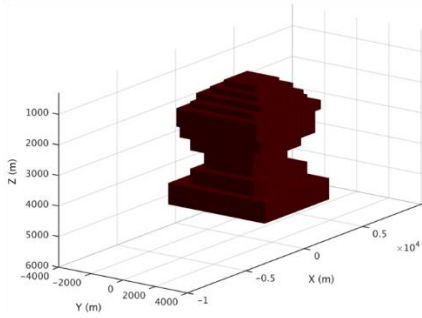


Figure 3: Model 2. A 3D view of the salt dome structure within the sea-bottom sediments.

Synthetic model study of the inversion algorithm based on hybrid FD-IE method

We have considered a salt dome in order to test the inversion method (Model 2 shown in Figure 3), which consists of a 300 m seawater layer with a resistivity of 0.3 Ohm-m, and a 10 Ohm-m half-space of sediments. A salt dome structure is embedded in the sediments, and it is located at a depth from 700 m below the sea floor down to 5000 m with a resistivity of 300 Ohm-m as shown in Figure 3. The synthetic in-line electric field data at frequencies of 1, 2, and 3 Hz were computed in 14 receivers from -7 km to 7 km in the x direction located 5 m above the sea floor. The transmitter line was positioned 45 m above the receiver line from -17 km to 17 km in the x direction. The synthetic observed data were generated by the 3D IE method, and were contaminated with random Gaussian noise having source-moment-normalized amplitude up to 10^{-14} V/Am².

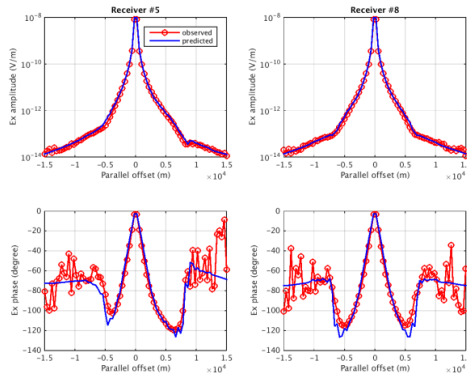


Figure 4: Examples of the data fit by the MCSEM inversion based on a salt dome model. The red lines represent the observed data, while the blue lines correspond to the predicted data.

The inversion domain was discretized using uniform rectangular grid with the cell size of 200 m x 500 m in the x and y directions, respectively. This grid has 30 layers in the z direction with the thickness logarithmically increasing

from 20 m to 500 m down until 5000 m depth below the sea bottom. The FD modeling domain was designed by padding all sides of the inversion domain with 8 more layers logarithmically increasing in size.

The inversion was terminated when the RMS misfit reached about 1, which was in good agreement with the level of the noise in the data. Figure 4 shows an example of the observed and predicted data at this misfit level. Figure 5 presents the inversion result at this misfit level. As one can see, we can find a very good shape of the upper part of the salt dome, but its bottom part cannot be recovered because the depth of the bottom (approximately 3000 m) is beyond the sensitivity of the data. This modeling study illustrates the practical effectiveness of the developed inversion algorithm based on the hybrid FD-IE method.

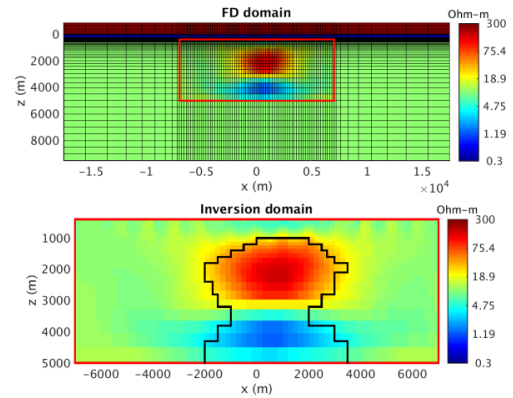


Figure 5: The resistivity distribution recovered by the inversion of MCSEM data based on a salt dome model. The top panel shows the FD modeling domain and discretization grid. The bottom panel shows the inversion result within the inversion domain only.

Conclusions

We have developed a novel 3D modeling and inversion approach, which combines the advantages of the finite difference (FD) and integral equation (IE) methods. This method was carefully validated by comparing the results with a conventional FD, a 1D semi-analytical solution, and a 3D IE solution. We have also developed an algorithm of 3D inversion for MCSEM data based on the novel hybrid FD-IE method. The developed inversion method was demonstrated in synthetic model study. The inverse geoelectrical images produced by the hybrid FD-IE inversion method agree well with the true model.

Acknowledgments

The authors acknowledge the support of the University of Utah Consortium for Electromagnetic Modeling and Inversion (CEMI), and TechnoImaging. Special thanks are extended to Dr. Endo, Dr. Cuma, and Dr. Cox for providing valuable comments.

Alumbaugh, D. L., G. A. Newman, L. Prevost, and J. N. Shadid, 1996, Three dimensional, wideband electromagnetic modeling on massively parallel computers: *Radio Science*, **31**, 1-23.

Amestoy, P. R., I. S. Duff, J.-Y. L'Excellent, and J. Koster, 2001, A fully asynchronous multifrontal solver using distributed dynamic scheduling: *SIAM Journal on Matrix Analysis and Application*, **23**, 15-31, doi: 10.1137/S0895479899358194.

Amestoy, P. R., A. Guermouche, J.-Y. L'Excellent, and S. Pralet, 2006, Hybrid scheduling for the parallel solution of linear systems: *Parallel Computing*, **32**, 136--156, doi: 10.1016/j.parco.2005.07.004.

Avdeev, D. B., 2005, Three-dimensional electromagnetic modeling and inversion from theory to application: *Surveys in Geophysics*, **26**, 767-799.

Cox, L. H., and M. S. Zhdanov, 2014, 3D airborne electromagnetic inversion using a hybrid edge-based FE-IE method with moving sensitivity domain: 84st Annual International Meeting, SEG, Expanded Abstracts, 739-744.

Gribenko, A., and M. S. Zhdanov, 2007, Rigorous 3D inversion of marine CSEM data based on the integral equation method: *Geophysics*, **72**, 229-254, doi: 10.1190/1.2435712.

Hursán, G., and M. S. Zhdanov, Contraction integral equation method in three-dimensional electromagnetic modeling, *Radio Sci.*, **37**(6), 1089, doi:10.1029/2001ES002513, 2002.

Newman, G. A., and D. L. Alumbaugh, 1995, Frequency domain modeling of airborne electromagnetic responses using staggered finite differences: *Geophysical Prospecting*, **43**, 1021-1042.

Tikhonov, A. N. and V. Y. Arsenin, 1977, *Solution of ill-posed problems*: V. H. Winston and Sons.

Wang, T., and G. W. Hohmann, 1993, A finite difference time-domain solution for three-dimensional electromagnetic modeling: *Geophysics*, **58**, 797-809.

Ward, S. H., and G. W. Hohmann, 1988, *Electromagnetic theory for geophysical applications: Electromagnetic methods in applied geophysics*, 130-311.

Yee, K., 1966, Numerical solution of initial boundary value problems involving Maxwell's equations in isotropic media: *IEEE Transactions on Antennas and Propagation*, **14**, 302-307, doi: 10.1109/TAP.1966.1138693.

Zhdanov, M. S., and G. Keller, 1994, *The geoelectrical methods in geophysical exploration*: Elsevier.

Zhdanov, M. S., 2002, *Geophysical inverse theory and regularization problems*: Elsevier.

Zhdanov, M. S., S. K. Lee, and K. Yoshioka, 2006, Integral equation method for 3D modeling of electromagnetic fields in complex structures with inhomogeneous background conductivity: *Geophysics*, **71** (6), 333-345.